Doubling dolutegravir dosage reduces the viral reservoir in ART-treated people with HIV

Céline Fombellida-Lopez[1,2], Aurelija Valaitienė[2], Lee Winchester[3], Nathalie Maes[4], Patricia Dellot[5], Céline Vanwinge[6], Aurélie Ladang[7], Etienne Cavalier[7], Fabrice Susin[8], Dolores Vaira[8], Marie-Pierre Hayette[8], Catherine Reenaers[9], Michel Moutschen[1,5], Courtney V. Fletcher[3], Alexander O. Pasternak[2]*, Gilles Darcis[1,5]*

[1]Laboratory of Immunology and Infectious Diseases, GIGA-Institute, University of Liège, Liège, Belgium; [2]Laboratory of Experimental Virology, Department of Medical Microbiology, Amsterdam UMC, University of Amsterdam, Amsterdam, The Netherlands; [3]Antiviral Pharmacology Laboratory, University of Nebraska Medical Center, Omaha, NE, USA; [4]Department of Biostatistics and Medico-Economic Information, University Hospital of Liège, Liège, Belgium; [5]Department of General Internal Medicine and Infectious Diseases, University Hospital of Liège, Liège, Belgium; [6]GIGA Flow Cytometry Platform, University of Liège, Liège, Belgium; [7]Department of Clinical Chemistry, University Hospital of Liège, Liège, Belgium; [8]Laboratory of Clinical Microbiology, University Hospital of Liège, Liège, Belgium; [9]Department of Gastroenterology, University Hospital of Liège, Liège, Belgium

*These authors contributed equally to the work and share the last authorship

Correspondence to Gilles Darcis (gdarcis@chuliege.be) and Alexander O. Pasternak (a.o.pasternak@amsterdamumc.nl)

Abstract

Whether antiretroviral therapy (ART) is always completely suppressive, or HIV might continue to replicate at low levels despite ART in some people with HIV (PWH), is still debated. Here, we intensified the ART regimen by doubling dolutegravir (DTG) dosage and investigated the impact of this strategy on HIV blood and tissue reservoirs, immune activation, and inflammation. Twenty HIV-infected adults, who had received a triple ART consisting of 50mg DTG/600 mg abacavir/300 mg lamivudine pre-intensification and had been suppressed on ART for at least two years, were enrolled in a phase 2 randomized clinical trial. Half of them received an additional 50 mg of DTG for a period of 84 days. As expected, plasma and tissue DTG concentrations significantly increased during the study period in the intensified group but not in the control group. Accordingly, significant decreases in total HIV DNA, intact HIV DNA, and cell-associated unspliced (US) HIV RNA in PBMCs, as well as in the US RNA/total DNA ratio, were observed in the intensified group but not in the control group. Intensification also modestly reduced markers of immune activation and exhaustion but had no measurable impact on systemic or tissue inflammation. Together with this, intensification resulted in a temporary decrease in the CD4/CD8 ratio that returned to baseline by day 84. Our results strongly suggest that the pre-intensification ART regimen was not completely suppressive. If confirmed in larger clinical trials, these results could have an impact on the clinical management of PWH and HIV curative strategies.

Introduction

Human immunodeficiency virus (HIV) remains a major global public health issue, with an estimated 39.9 million people with HIV (PWH) at the end of 2023. Out of them, 30.7 million (77%) were accessing antiretroviral therapy (ART) (https://www.unaids.org/en/resources/fact-sheet). ART suppresses plasma viral load to undetectable levels, restores immune function, and eliminates the risk of developing AIDS (1). Current ART usually consists of one or two nucleotide or nucleoside reverse transcriptase inhibitors and the second or third drug of another class (e.g., a non-nucleoside reverse transcriptase inhibitor, a protease inhibitor (PI), or an integrase strand transfer inhibitor (INSTI)) (https://eacs.sanfordguide.com/). The mechanism of action of ART is interfering with different steps of the viral replication cycle, such as reverse transcription, integration, or viral particle maturation. Importantly, ART only blocks the infection of new cells and does not inhibit HIV gene expression in cells that were infected prior to ART initiation or in the progeny of such cells (2).

ART is not curative, and the main barrier to an HIV cure is the presence of latent viral reservoirs that arise due to the ability of HIV to integrate its genome into the host chromosome and persist in a latent form in some of the cells it infects, such as memory CD4+ T cells (3, 4). These reservoir cells harbour stably integrated and replication-competent provirus that can reactivate and, after cessation of ART, fuel a rapid viral rebound (5). HIV reservoirs persist lifelong, slowly decaying over time (6-8). Several mechanisms have been described to explain the long-term persistence of HIV reservoirs, including the infection of long-lived CD4+ T cells and clonal expansion by homeostatic or antigen-driven cellular proliferation or by HIV integration in or near genes that promote cellular proliferation (9, 10). However, if therapy does not prevent all new infections, then replenishment by *de novo* virus replication provides an additional potential mechanism of reservoir persistence (11).

Whether ART is fully suppressive is a topic of considerable and long-standing debate (12). Evidence of residual replication in ART-suppressed PWH has been previously presented (13-16), but other groups published reports that contest this notion (17-20). One strong argument against ongoing viral replication is the absence of detectable virus evolution on ART. However, if residual replication occurs intermittently and at a low level, with short infection chains continuously arising and terminating, then nucleotide substitutions are expected to be sporadic and not linked by temporal structure, unless the sampling is very deep and intensive (13, 21). In principle, failure to detect virus evolution does not form an unequivocal proof that residual

viral replication does not occur at all: absence of evidence is not evidence of absence. Indeed, Paryad-Zanjani et al. recently developed a mathematical model to track the viral dynamics in lymph nodes (LNs) after the initiation of ART (22), which suggested that the methods used by the previous studies to detect genetic divergence were not sufficiently sensitive and that these studies would have been unlikely to detect residual replication.

Over time, this persistent low-level residual replication may contribute to chronic immune activation and inflammation in ART-treated PWH (23). Constant stimulation of the immune system could lead to immune exhaustion and premature immune senescence, resulting, over the years, in the development of non-AIDS co-morbidities, such as cardiovascular disease (24). This replication may occur in anatomical sanctuaries/compartments, notably the LNs and the gut-associated lymphoid tissue (GALT), two sites massively infected by HIV (25). Lower penetration of antiretroviral drugs to these tissues reduces the local drug concentrations and, consequently, their effectiveness in preventing HIV replication (26-28).

One way to investigate the residual replication is to intensify a standard ART regimen and measure the impact of this intensification on latent reservoirs, inflammation, and immune activation. If a reduction of a virological parameter is observed, it would strongly suggest that the ART regimen prior to intensification did not completely prevent virus replication. Several groups have conducted ART intensification trials, either by adding a CCR5 antagonist (maraviroc) or an INSTI (raltegravir or dolutegravir (DTG)) to a standard three-drug regimen. Some of these trials have indeed revealed residual virus replication at baseline, as treatment intensification caused a decrease in immune activation, a decrease in cell-associated HIV RNA in the ileum, and a transient increase in 2-long terminal repeat (2-LTR) circles (29-38). However, other groups have failed to demonstrate any effects of ART intensification on virological parameters (39-45).

In summary, is still unclear whether ongoing viral replication can occur in the presence of ART. The consequences of residual replication for the HIV curative strategies are important since approaches aimed at eliminating viral reservoirs such as latency reversal ("shock-and-kill") (46) are not expected to be fully effective if the virus continues to replicate despite treatment. In the worst-case scenario, the residual replication could lead to significant replenishment of the HIV reservoir upon latency reversal, compensating for any reservoir depletion achieved by this strategy. Therefore, understanding the phenomenon of residual replication and developing strategies to eliminate it are key elements in the quest to cure PWH.

111 Here, we intensified ART in PWH who had been suppressed on ART for at least two years, by
112 doubling the dosage of DTG, an antiretroviral drug that had already been part of the regimen
113 pre-intensification. We investigated the impact of this intensification on HIV blood and tissue
114 latent reservoirs, immune activation, and inflammation.

115

116 **Results**

117 **Study design and participants**

118 Between February and July 2019, twenty ART-suppressed participants receiving a triple
119 antiretroviral regimen consisting of 50 mg DTG, 600 mg abacavir (ABC), and 300 mg
120 lamivudine (3TC) daily were enrolled into two groups as follows: 10 participants continued to
121 receive this regimen (control group) and 10 participants received an additional 50 mg of DTG
122 daily for 84 days (intensified group) as shown in Figure S1. Study participants were mostly
123 Caucasian males and the median age was 52 years. The median cumulative time of viral
124 suppression on ART was 7.4 years and participants had maintained continuous viral
125 suppression for a median of 3.9 years before the study. The clinical characteristics of the
126 participants at baseline are shown in Table 1.

127

128 **ART intensification increases plasma and tissue DTG concentrations**

129 To assess if the desired experimental conditions were achieved, we monitored the
130 concentrations of DTG and 3TC, two antiretroviral drugs that were part of the ART regimen
131 (Figure 1, Figure S2). Baseline plasma and rectal tissue DTG and 3TC concentrations were not
132 significantly different between the intensified and control groups (Table 1). At median, baseline
133 DTG concentration in the rectal tissue was 16.7% (interquartile range (IQR), 15.1%-24.6%) of
134 the corresponding DTG plasma concentration, strikingly close to the value (17%) reported
135 previously (47). As expected, plasma and tissue DTG concentrations significantly increased
136 between days 0 and 84 in the intensified group but not in the control group (Figures 1A, 1B).
137 In fact, DTG concentrations almost exactly doubled in plasma (median fold increase, 1.97-
138 fold) and more than doubled in tissue (median fold increase, 2.48-fold) on day 84, as compared
139 to day 0, in the intensified group. However, at day 84, tissue DTG concentration in the
140 intensified group was still much lower (median, 20.0%; IQR, 17.3%-22.3%) than the
141 corresponding DTG plasma concentration, reflecting limited penetration of DTG into the

142 tissue. Plasma and tissue 3TC concentrations did not change on day 84 compared to day 0 in
143 both groups, which was expected as the dosage of 3TC was not increased in any group (Figures
144 1C, 1D). However, we did observe a transient increase in the plasma DTG concentration in the
145 control group and in the plasma 3TC concentration in both groups on days 1 and 56 of the study
146 (Figure S2), with the concentrations returning to baseline levels by day 84. One possible
147 explanation for this effect could be an increased adherence of the participants to their ART
148 regimens during the study ("white coat compliance") (48).

149

150 **ART intensification reduces HIV reservoir**

151 To investigate the effect of treatment intensification on the viral reservoir, we longitudinally
152 measured total HIV DNA and cell-associated unspliced (US) HIV RNA in peripheral blood
153 mononuclear cells (PBMCs) on days 0, 1, 28, 56, and 84 of the study. In addition, we measured
154 intact HIV DNA in PBMCs and total HIV DNA in rectal biopsies on days 0 and 84 of the study.
155 Strikingly, we observed significant longitudinal decreases in total HIV DNA, US RNA, and
156 HIV transcription level per provirus (US RNA/total DNA ratio) in PBMCs in the intensified
157 group ($p=0.0022$, $p<0.001$, and $p<0.001$, respectively) but not in the control group, with
158 significant differences in the relative changes from baseline for two of these three markers
159 between the groups ($p<0.001$, $p=0.010$, and $p=0.090$, respectively) (Figures 2A-2C, Figures
160 S3-S5). While total HIV DNA in the intensified group transiently decreased in the first 28 days
161 of the study (median (IQR) fold decrease from day 0 to day 28, 2.1 (1.1-4.7) fold, $p=0.027$)
162 and increased afterwards (Figure 2A, Figure S3), US RNA and US RNA/total DNA ratio in the
163 intensified group continued to decrease throughout the whole study period (Figures 2B-2C,
164 Figures S4, S5). By day 84, US RNA and US RNA/total DNA ratio have decreased from day
165 0 by medians (IQRs) of 5.1 (3.3-6.4) and 4.6 (3.1-5.3) fold, respectively ($p=0.016$ for both
166 markers). In comparison, in the control group these markers remained at the baseline level or
167 even increased (Figures 2A-2C). These effects were confirmed by measurement of intact HIV
168 DNA in PBMCs that was quantified by the intact proviral DNA assay (IPDA) (49). We
169 measured a significant decrease in the intact HIV DNA between days 0 and 84 in the intensified
170 group (median (IQR) fold decrease, 2.2 (1.3-3.1) fold, $p=0.039$) but not in the control group
171 (Figure 2D). In contrast, total HIV DNA in rectal tissue did not change between days 0 and 84
172 in both groups (Figure 2E). Taken together, these results indicate that the intensification
173 reduced the HIV reservoir in the peripheral blood of ART-treated PWH.

174

175 **ART intensification modestly reduces markers of immune activation and exhaustion**

176 To detect if intensification had an impact on immune activation and exhaustion, we performed
177 longitudinal flow cytometry analysis to assess the expression of cell surface markers of
178 activation (HLA-DR, CD38) and exhaustion (PD-1, TIGIT) on CD4+ and CD8+ T cells (Figure
179 3, Figure S6). A transient but significant increase in the percentage of CD4+ cells expressing
180 PD-1 (p=0.022), and a significant decrease in the percentage of CD8+ cells expressing CD38
181 (p=0.034) were measured in the control group. A decrease in the percentage of CD4+ cells
182 expressing TIGIT was measured in the intensified group (p=0.031), with a significant
183 difference compared to the control group (p=0.048). We also measured a modest yet significant
184 decrease in the percentage of CD8+ cells co-expressing CD38 and HLA-DR in the intensified
185 group (p=0.049) (Figure 3). Overall, these results indicate that intensification modestly reduced
186 markers of immune activation and exhaustion.

187

188 **ART intensification does not impact systemic or tissue inflammation**

189 To investigate the effect of intensification on systemic and tissue inflammation, we quantified
190 several inflammatory cytokines in plasma and in rectal tissue. In plasma, we longitudinally
191 measured the levels of IL-1β, IL-6, IFN-γ, IL-17 α, and TNF-α, and in rectal tissue, we
192 measured expression of the same cytokines by quantifying their mRNA levels at days 0 and
193 84. We observed a significant increase in plasma IL-6 levels in the control group (p=0.049).
194 Apart from that, no significant change from baseline for any cytokine was observed for both
195 groups in both plasma and tissue (Figure 4, Figure S7). Overall, these results indicate that
196 intensification did not measurably impact systemic or tissue inflammation.

197

198 **ART intensification leads to a transient decrease in the CD4/CD8 ratio**

199 We longitudinally measured CD4 and CD8 T-cell counts, CD4/CD8 ratio, as well as plasma
200 levels of soluble CD14 (sCD14), a marker of monocyte/macrophage activation, and of C-
201 reactive protein (CRP), an inflammation marker (Figure 5, Figure S8). No significant changes
202 were observed in the CD4 and CD8 counts in both groups, however we measured a transient
203 but significant decrease in the CD4/CD8 ratio in the intensified group (p=0.0081) that returned

204 to the baseline level by day 84 (Figure 5). No change in the CD4/CD8 ratio was observed in
205 the control group. We also observed a significant decrease in the sCD14 level in the control
206 group ($p<0.001$) and a trend toward an increase in the intensified group ($p=0.079$), which
207 resulted in a significant difference between the groups ($p<0.001$). Finally, we observed a small
208 but significant increase in the CRP level in the control group ($p=0.045$) but not in the intensified
209 group.

210

211 **Correlations between the measured parameters**

212 Finally, we assessed pairwise correlations between the measured parameters at baseline, as well
213 as between their time-weighted changes from baseline during the study (time-weighted areas
214 under curve) and between their relative changes between days 0 and 84 of the study (Figures
215 S9-S11). At baseline, we found strong positive pairwise correlations between the levels of
216 different plasma inflammatory cytokines, as well as between the percentages of peripheral
217 CD8+ T cells expressing TIGIT and inflammatory cytokine levels in plasma and tissue. Of the
218 latter, especially strong correlations were observed between CD8+TIGIT+ cell percentages and
219 plasma or tissue levels of IL-6 (*rho*=0.74 and *rho*=0.71, respectively; $p<0.001$). We also found
220 positive correlations at baseline between US RNA/total DNA ratio and percentages of CD4+ T
221 cells expressing CD38 and co-expressing CD38 and HLA-DR, markers of immune activation
222 (*rho*=0.53, p=0.020 and *rho*=0.50, p=0.023, respectively). Furthermore, US RNA changes
223 between days 0 and 84 positively correlated with changes in levels of expression of immune
224 activation/exhaustion markers CD38+ on CD4+ cells and PD-1+ on CD8+ cells (*rho*=0.53,
225 p=0.030 and *rho*=0.61, p=0.011, respectively) and of tissue inflammatory cytokine IL-1β
226 mRNA (*rho*=0.62, p=0.0096). These correlations were even stronger for the changes between
227 days 0 and 84 of US RNA/total DNA ratio (CD4+CD38+: *rho*=0.55, p=0.029; CD8+PD-1+:
228 *rho*=0.73, p=0.0018; IL-1β mRNA: *rho*=0.76, p=0.0011). This confirms the results of our
229 earlier study, where US RNA/total DNA ratio was found to correlate with markers of immune
230 exhaustion (50). Interestingly, intact, but not total, HIV DNA in PBMCs strongly negatively
231 correlated with time of viral suppression (*rho*=-0.67, p=0.0016), confirming earlier
232 observations that intact HIV DNA decays on ART much faster than the defective (or total) HIV
233 DNA (51, 52).

234

235

236 **Discussion**

237 The aim of this study was to investigate whether ongoing viral replication contributes to HIV
238 persistence under ART. To the best of our knowledge, this is the first study where ART
239 intensification was achieved not by adding a new antiretroviral drug to the existing regimen
240 but by increasing the dosage of a drug that was already part of the regimen pre-intensification.
241 We evaluated the impact of doubling the dosage of DTG on HIV cellular and tissue reservoirs,
242 immune activation, exhaustion, and inflammation in ART-suppressed PWH.

243 As expected, plasma and tissue DTG concentrations significantly increased between day 0 and
244 day 84 in the intensified group but not in the control group. Accordingly, significant decreases
245 in total HIV DNA, intact HIV DNA, US HIV RNA, and US RNA/total DNA ratio in PBMCs
246 were observed during the study period in the intensified group but not in the control group.
247 This strongly suggests that the pre-intensification ART regimen was not completely
248 suppressive. The transient decrease in total DNA at day 28 may have been due to an initial
249 decrease in newly infected cells upon ART intensification, however at the subsequent time
250 points this effect was likely masked by proliferation (clonal expansion) of infected cells, mostly
251 containing defective proviruses. In line with this, the number of intact proviruses decreased,
252 but that of total proviruses did not change, between days 0 and 84 (Figures 2A, 2D).

253 In addition, intensification modestly yet significantly reduced percentages of CD4+ T cells
254 expressing TIGIT, a T-cell exhaustion marker (53), and percentages of CD8+ T cells co-
255 expressing CD38 and HLA-DR, T-cell activation markers. Interestingly, CD4+ cells expressing
256 TIGIT have been shown to be enriched for HIV persistence in ART-treated PWH (54).
257 Arguably, the reduction of HIV reservoir upon intensification has caused a corresponding
258 reduction in chronic immune activation and exhaustion in this cohort. Indeed, changes in US
259 HIV RNA levels and US RNA/total DNA ratio during the study positively correlated with
260 changes in levels of markers immune activation, exhaustion, and inflammation, suggesting a
261 link between changes in HIV reservoir activity and levels of immune activation and
262 inflammation. These results are in line with previous studies reporting decreases in immune
263 activation markers upon ART intensification (32-35).

264 In contrast, in the control group we measured significant longitudinal increases in total HIV
265 DNA, percentages of CD4+ T cells expressing PD-1, another T-cell exhaustion marker, and in
266 the plasma levels of IL-6, an inflammatory cytokine, and of CRP, another marker of
267 inflammation. Residual HIV replication, among other factors, could have contributed to these

268 effects in the control group. However, in the control group we also observed a reduction in the
269 percentages of CD8+ T cells co-expressing a T-cell activation marker CD38 and a strong
270 reduction in the plasma levels of sCD14. One possible explanation for these effects can be
271 increased adherence of the participants to their ART regimens during the study.

272 Two previous studies have measured a transient increase in HIV episomal DNA (2-LTR circles)
273 upon ART intensification with raltegravir, an INSTI (31, 36). As 2-LTR circles are a byproduct
274 of HIV integration and are expected to accumulate if integration is blocked, this was interpreted
275 as a strong evidence of new infections pre-intensification. However, another study did not
276 observe any change in 2-LTR circles upon ART intensification with DTG (45). In our study,
277 despite repeated attempts using different assays, we could only detect 2-LTR circles in a small
278 minority of participants (<5%) (data not shown). Notably, the effects of intensification on 2-
279 LTR circles in these previous studies were much more pronounced in participants who had
280 been treated with a PI-based ART regimen pre-intensification (31, 36). As PI-based regimens
281 have been shown to be less suppressive than other ART regimens (16, 55-57), they might have
282 allowed for a higher level of new infections and consequently of 2-LTR circles in these studies.

283 In contrast, in our study, participants had been treated with a DTG-based regimen for at least
284 two years and had had a suppressed plasma viral load (<50 copies/mL) for at least 2 years 11
285 months pre-intensification. Plausibly, the lack of detectable 2-LTR circles in our participants
286 reflects the high potency of their ART regimens and a long period of virological suppression
287 before the study. Remarkably, the intensification revealed that even this highly potent regimen
288 was not completely suppressive. Thus, our results emphasize that 2-LTR circles are not a very
289 sensitive marker of new infections due to their relative scarcity in infected cells. 2-LTR circles
290 represent only ~10% of total episomal DNA (58) and are not expected to be present in every
291 newly infected cell. In contrast, a newly infected CD4+ T lymphocyte can contain hundreds to
292 thousands of US HIV RNA copies on the peak of infection (59). Therefore, a change in the US
293 RNA level upon ART intensification is a much more sensitive indicator of new infections than
294 that of 2-LTR circles, as confirmed by this study.

295 Due to low penetration of antiretroviral drugs into tissue sites and anatomic sanctuaries (26-
296 28, 60, 61), ART pressure on HIV replication is generally expected to be more relaxed in tissues
297 than in peripheral blood. However, we did not observe any effect of the intensification on total
298 HIV DNA in the rectal tissue. Although DTG concentration in the rectal tissue did increase
299 upon intensification, it remained much lower than in the peripheral blood. This possibly

300 contributed to the lack of detectable effect of intensification on the HIV DNA in tissue.
301 Alternatively, intensification with DTG, an INSTI, had no effect in the tissue due to the
302 preponderance of abortive infection events in lymphoid tissues that occur by cell-to-cell contact
303 and are terminated prior to integration (62, 63). It is also possible that, similarly to the
304 peripheral blood, the effect of the intensification on the reservoir in tissue was masked by the
305 clonal expansion of defective proviruses by day 84 of the study.

306 The majority of previous studies that used INSTIs (raltegravir or DTG) as intensification drugs
307 added it as a fourth drug using the standard dosage. For example, the DTG dosage in the study
308 of Rasmussen et al. was 50 mg daily (45). In our study, we used a twice-higher dosage (100
309 mg daily). This DTG dosage is commonly used in clinical practice. Indeed, in PWH with
310 confirmed or clinically suspected resistance to the integrase inhibitor class, the recommended
311 dosage of DTG is 50 mg twice daily (https://www.cbip.be/fr/chapters/12?frag=10868). Based
312 on our results (and pending the confirmation by larger studies), an increased dosage of DTG
313 might be warranted in the future as a part of a standard regimen even in PWH without
314 resistance. However, this has to be approached with caution as intensification has caused a
315 transient decrease in the CD4/CD8 ratio in our study.

316 The main strength of our study is the measurement of a large number of virological and
317 immunological parameters that allowed us to observe a significant impact of intensification on
318 both virus and host. Our study is the first to observe significant reductions in as many as four
319 HIV markers following ART intensification. Moreover, we measured plasma and tissue
320 concentrations of DTG, allowing us to directly demonstrate their increase upon intensification.
321 Our results are in line with some earlier studies that reported a decrease in cell-associated HIV
322 RNA or a transient increase in 2-LTR circles upon intensification (31, 32, 36). However, they
323 are in contrast with other studies, in which treatment intensification did not affect HIV markers
324 (39, 40, 42). As this is the first ART intensification study to increase the dosage of an existing
325 antiretroviral drug instead of adding a new drug, the results of this study and those of previous
326 intensification studies cannot be directly compared.

327 Some limitations can be highlighted. First, we included twenty PWH (ten participants per arm).
328 Although this small sample size does somewhat limit the robustness of the conclusions, we
329 would like to emphasize that in this cohort, we performed a very detailed analysis,
330 longitudinally measuring 30 biomarkers at five time points during ART. Secondly, despite the
331 randomization, the groups were still not perfectly balanced as levels of total HIV DNA in

332 PBMCs were by chance higher at baseline in the intensified group. However, this is unlikely
333 to have affected the conclusions of the study because (i) this study has a within-subject
334 (repeated-measures) design, with the longitudinal change of a parameter within the same
335 participant during the study being the main outcome, and (ii) this difference most probably
336 reflects a higher number of infected cells, and not a higher level of residual replication, at
337 baseline in the intensified group. No significant differences between the groups were found at
338 baseline in the levels of the other four virological markers we measured (US RNA in PBMCs,
339 US RNA/total DNA ratio, intact DNA in PBMCs, and total DNA in tissue), as well as between
340 the antiretroviral drug concentrations in plasma or in tissue. The lack of blinding and placebo
341 control, the predominantly male study population, and the absence of post-intervention follow-
342 up represent additional limitations of our study. Moreover, these findings should be considered
343 exploratory and hypothesis-generating, warranting confirmation in larger, placebo-controlled,
344 and blinded trials. Nevertheless, we believe that the convergence of the effect of intensification
345 on multiple reservoir markers in the same direction indicates a potentially meaningful
346 biological signal that merits further investigation.

347 In conclusion, doubling the DTG dosage in PWH who had been suppressed on DTG-containing
348 ART for a number of years resulted in a reduction in the levels of four HIV reservoir markers
349 in peripheral blood, as well as in markers of T-cell activation and exhaustion. If confirmed in
350 larger clinical trials, these results could have an impact on the clinical management of PWH.
351 Moreover, if ongoing viral replication does indeed replenish HIV reservoirs over time, then
352 improving ART regimens should be a necessary part of the curative strategies.

353

354 **Methods**

355 **Study design and participants**

356 This was a phase 2 open-label, interventional, monocentric, randomized, and controlled clinical
357 trial performed at the Hospital University of Liège (Belgium) in which 20 HIV-infected adults
358 were enrolled. Eligible participants had been treated with a combination of 50 mg DTG, 600
359 mg ABC, and 300 mg 3TC for more than two years and the purpose of this study was to assess
360 the impact of DTG intensification (an additional daily dose of 50 mg) compared to a control
361 group that continued with the above regimen. This study was a proof-of-concept trial designed
362 to reveal biological effects of ART intensification and the primary outcome was defined as "to
363 evaluate the impact of treatment intensification at the level of total and replication-competent

364 reservoir in blood and in tissues", with a time frame of 3 months. Participants were required to
365 have a plasma viral load suppressed below 20 HIV RNA copies/mL during the 12 months
366 before screening (allowing "blips") and an absolute CD4+ T lymphocyte count above 200
367 cells/mm^3. One participant out of 20 had an isolated "blip" of 115 copies/mL nine months
368 before the study initiation. The detailed inclusion and exclusion criteria can be found in the
369 supplementary data (Supplementary data 1). The study was approved by the Liège University
370 Hospital-Faculty Ethics Committee (Comité d'Éthique Hospitalo-Facultaire Universitaire de
371 Liège, 2018/228). Prior to inclusion in the study, each participant had dated and signed an
372 informed consent form. ClinicalTrials.gov identifier: NCT05351684.

373 Historical plasma HIV RNA measurements, CD4+ T-cell counts, and treatment data were
374 retrieved from the outpatient medical records. The duration of continuous virological
375 suppression was calculated as the duration of the latest period with undetectable plasma HIV
376 RNA prior to the study initiation, allowing isolated 'blips' of 50–999 copies/ml. The duration
377 of cumulative suppression was calculated by adding together all such periods of continuous
378 suppression.

379

380 **Clinical procedures**

381 Each participant was randomly assigned to the intensified group or to the control group. This
382 study lasted 84 days in which 5 visits were programmed (days 0, 1, 28, 56, and 84). One visit
383 prior to inclusion was added to perform a blood test to ensure that the participant met the
384 inclusion/exclusion criteria for the study. The blood test included blood and platelet count,
385 electrolyte panel, creatinine, LDH counts, liver tests, coagulation tests, CD4 and CD8
386 lymphocyte counts and a plasma viral load. β-HCG levels were measured in women at each
387 visit to ensure that they were not pregnant. All participants completed the 12 week-long study
388 and no individuals were lost to follow-up.

389 Safety and tolerability evaluations were conducted on day 28 and day 84 and included a clinical
390 examination and routine laboratory testing (liver function tests, kidney function, and complete
391 blood count). Medication adherence was also monitored through pill counts performed by the
392 study nurses.

393 No virological blips above 50 copies/mL were observed and no adverse events were reported
394 by participants during the 3-month intensification period. Although CPK levels were not

395 included in the routine biological monitoring, no participant reported muscle pain or other
396 symptoms suggestive of muscle toxicity.

397 Blood samples were collected in 4 EDTA tubes (~40mL) at days 0, 1, 28, 56, and 84 and directly
398 sent to the AIDS reference laboratory of Liège University Hospital for PBMC isolation. PBMC
399 samples were stored at -150°C for measurements of the HIV reservoir and immunological
400 parameters. Plasma samples were used to measure soluble inflammation markers. Ten flash-
401 frozen rectal biopsies were collected on days 0 and 84 during a routine gastroenterology visit.
402 The cryotubes containing the biopsies were directly placed in liquid nitrogen and stored at -
403 150°C.

404

405 **PBMC isolation**

406 PBMCs were isolated from whole blood by density gradient centrifugation using Ficoll-
407 Paque® Plus. The blood samples were collected in EDTA tubes and centrifuged at 1200 X g
408 for 10 min (acceleration 9, brake 9). The plasma was removed and stored at -150°C. The blood
409 was then well homogenized with RPMI 1640, gently transferred in a Falcon tube that contained
410 12,5 mL of Ficoll, and centrifuged at 700 X g for 20 minutes (acceleration 6, brake 0). The
411 PBMC layer was removed, diluted in 50 mL RPMI 1640, and centrifuged at 300 X g for 7
412 minutes (acceleration 9, brake 9). The supernatant was removed, and the process was repeated
413 two more times, completing three washes. The pellet was resuspended, and the cells were
414 counted. Foetal bovine serum (FBS) was added to the re-suspended pellet to obtain $10x10^6$
415 cells/500 µL. For cryopreservation, 500 µL of freeze mixture (10% DMSO in FBS) was added
416 to 500 µL of the cell suspension in the cryotubes. Cryotubes were slowly frozen in the Mr.
417 Frosty™ freezing container at -80 °C and transferred to -150°C the next day.

418

419 **Quantification of total HIV DNA and cell-associated US HIV RNA in PBMCs**

420 Total nucleic acids were extracted from $2x10^6$ PBMCs using Boom isolation method (64). Total
421 HIV DNA was measured by qPCR using the previously described primer/probe combination
422 that amplifies the HIV packaging signal (Ψ) region (49). Extracted cellular RNA was treated
423 with DNase (DNA-free kit; ThermoFisher Scientific) to remove genomic DNA that could
424 interfere with the quantitation and reverse transcribed into cDNA using random primers and
425 SuperScript III reverse transcriptase (all from ThermoFisher Scientific). To quantify cell-

426 associated US HIV RNA, this cDNA was pre-amplified using primer pair Ψ_F (49) and HIV-
427 FOR (65). The product of this PCR was used as template for a seminested qPCR with the Ψ
428 primer/probe combination (49). HIV DNA or RNA copy numbers were determined using a 7-
429 point standard curve with a linear range of more than 5 orders of magnitude that was included
430 in every qPCR run and normalized to the total cellular DNA (by measurement of β-actin DNA)
431 or RNA (by measurement of 18S ribosomal RNA) inputs, respectively, as described previously
432 (66). Non-template control wells were included in every qPCR run and were consistently
433 negative. Total HIV DNA and US RNA were detectable in 90.7% and 66.7% of the samples,
434 respectively. Undetectable measurements of US RNA or total DNA were assigned the values
435 corresponding to 50% of the corresponding assay detection limits, with a maximum of 25
436 copies/μg total RNA or 50 copies/10^6 PBMCs, respectively. The detection limits depended on
437 the amounts of the normalizer (input cellular DNA or RNA) and therefore differed among
438 samples. Measurements with low input cellular DNA or RNA and undetectable total HIV DNA
439 or US RNA (n=2 and n=3, respectively), were excluded from the analysis. HIV transcription
440 levels per provirus (US RNA/total DNA ratios) were calculated taking into account that 10^6
441 PBMCs contain 1 μg of total RNA (67).

442

443 **Quantification of intact HIV DNA in PBMCs**

444 Intact HIV DNA was quantified on days 0 and 84 of the study by the IPDA (49). In brief,
445 genomic DNA was isolated from $4x10^6$ PBMCs using Puregene Cell Kit (QIAGEN Benelux
446 B.V.) according to the manufacturer's instructions and digested with *Bgl*I restriction enzyme
447 (ThermoFisher Scientific) as described previously (68). Notably, only a small minority (<8%)
448 of HIV clade B sequences contain *Bgl*I recognition sites between Ψ and *env* amplicons,
449 therefore *Bgl*I digestion is not expected to substantially influence the IPDA output, while
450 improving the assay sensitivity by increasing the genomic DNA input into a ddPCR reaction
451 (68). After desalting by ethanol precipitation, genomic DNA was subjected to two separate
452 multiplex droplet digital PCR (ddPCR) assays: one targeting HIV Ψ and *env* regions using
453 primers and probes described previously, including the unlabelled *env* competitor probe to
454 exclude hypermutated sequences (49), and one targeting the cellular *RPP30* gene, which was
455 measured to correct for DNA shearing and to normalize the intact HIV DNA to the cellular
456 input. The *RPP30* assay amplified two regions, with amplicons located at exactly the same
457 distance from each other as HIV Ψ and *env* amplicons. The first region was amplified using a

458 forward primer 5'-AGATTTGGACCTGCGAGCG-3', a reverse primer 5'-
459 GAGCGGCTGTCTCCACAAGT-3', and a fluorescent probe 5'-FAM-
460 TTCTGACCTGAAGGCTCTGCGCG-BHQ1-3' (69). The second region was amplified using
461 a forward primer 5'-AGAGAGCAACTTCTTCAAGGG-3', a reverse primer 5'-
462 TCATCTACAAAGTCAGAACATCAGA-3', and a fluorescent probe 5'-HEX-
463 CCCGGCTCTATGATGTTGTTGCAGT-BHQ1-3'. The ddPCR conditions were as described
464 previously (49) with some minor amendments: we used 46 cycles of
465 denaturation/annealing/extension and the annealing/extension temperature was 60°C. Intact
466 HIV DNA was detectable in 79.5% of the samples. Undetectable measurements of intact HIV
467 DNA were assigned the values corresponding to 50% of the assay detection limits. The
468 detection limits depended on the amounts of the normalizer (input cellular DNA) and therefore
469 differed among samples. For two participants, in whom intact HIV DNA on day 0 was
470 undetectable due to a technical issue, we included day 1 values in the analysis. Excluding these
471 two participants did not change the conclusions (data not shown).

472

473 **Quantification of total HIV DNA in rectal biopsies**

474 Prior to total HIV DNA isolation, rectal biopsies were homogenized with the TissueLyser
475 (QIAGEN Benelux B.V.). Total HIV DNA was isolated using ReliaPrep™ gDNA Tissue
476 Miniprep System (Promega) according to the manufacturer's instructions. Total HIV DNA in
477 rectal biopsies was quantified using exactly the same method as total HIV DNA in PBMCs (see
478 above). Total HIV DNA was detectable in 92.5% of the rectal tissue samples. Undetectable
479 measurements of total HIV DNA were assigned the values corresponding to 50% of the
480 corresponding assay detection limits. The detection limits depended on the amounts of the
481 normalizer (input cellular DNA) and therefore differed among samples.

482

483 **Quantification of immune activation and exhaustion**

484 Flow cytometry was used to quantify surface markers of immune activation and exhaustion
485 (CD38, HLA-DR, PD-1, TIGIT) on CD4+ and CD8+ T cells. Cryopreserved PBMCs ($10x10^6$
486 cells) were thawed and stained with a fixable viability dye Zombie NIR (Sony), and the
487 following antibodies: CD3-APC/Fire810, CD4-PE/Fire700, CD8a-PercP (all from Sony), PD-
488 1-PE, TIGIT-BV421, HLA-DR-BB515, CD38-BV711 (all from BD Biosciences). Cells were

489 then washed, fixed in 1% paraformaldehyde, and run on a FACS SONY ID7000. Analysis was
490 performed using FlowJo software (v10.8.1). Cells were gated according to morphological
491 parameters (forward and side scatter) and viability. The complete gating strategy can be found
492 in the supplemental data (Fig. S12). To exclude the effect of inter-assay variation on the data,
493 samples from each participant were always analysed together.

494

495 **Quantification of systemic and tissue inflammation**

496 To quantify systemic inflammation, the levels of five plasma inflammatory cytokines (IFN-γ,
497 IL-1β, IL-6, IL-17α, TNF-α) were measured on MAGPIX (Luminex) using the ProcartaPlex™
498 Human Inflammation Panel, 20plex (ThermoFisher Scientific). sCD14 was quantified by
499 Human CD14 Quantikine ELISA Kit (R&D Systems). CRP was measured by high-sensitivity
500 C-reactive protein (hs-CRP) test.

501 To measure tissue inflammation, we determined rectal tissue levels of mRNAs encoding five
502 inflammatory cytokines (IL-1β, IL-6, IFN-γ, IL-17 α, and TNF-α). Rectal tissue biopsies were
503 manually homogenized and lysed in buffer L6 (64) and RNA was extracted using Boom
504 isolation method (64). Extracted RNA was treated with DNase (DNA-free kit; ThermoFisher
505 Scientific) and reverse transcribed using random primers and SuperScript III reverse
506 transcriptase (all from ThermoFisher Scientific). Cytokine mRNAs were quantified using
507 TaqMan Gene Expression Assays (all from ThermoFisher Scientific): IL-1β -
508 Hs01555410_m1, IL-6 - Hs00174131_m1, IFN-γ - Hs00989291_m1, IL-17 α -
509 Hs00174383_m1, TNF-α - Hs00174128_m1. Levels of cytokine mRNAs were normalized to
510 that of *GAPDH* mRNA, measured using a TaqMan Gene Expression Assay Hs02758991_g1.

511

512 **Quantification of antiretroviral drug concentrations**

513 Briefly, DTG was extracted from plasma samples via methanolic protein precipitation and from
514 tissue samples via tissue homogenization, followed by protein precipitation. A DTG standard
515 calibration curve over the range 20.0-5,000 ng/mL and stable isotope labelled internal standard
516 were used to generate an analyte/internal standard response. Analyte/internal standard response
517 was detected by liquid chromatography tandem mass spectrometry (LCMS) based on
518 previously described methods (26, 60, 70). Tissue penetration ratios of DTG were calculated
519 as the ratios of DTG concentrations in tissue (as ng/mL after conversion from ng/g by dividing

520 the values in ng/g by 1.06 (71)) to the concentrations in plasma (ng/mL). Lamivudine (3TC)
521 concentrations were determined with an LCMS method similar to our previously described
522 procedures (72). Differences are as follows: 3TC stock and standard working solutions were
523 prepared in methanol and demonstrated similar stability. The MS used was a triple-quadrupole
524 AB Sciex 5500 series monitoring positive ion transitions 230.1 -> 112.1 (3TC) and 233.1 ->
525 115.1 (stable labeled internal standard). Mobile phase was 12.5% acetonitrile and 0.1% formic
526 acid in deionized water. No source rinsing mobile phase was needed. The limit of quantitation
527 was 30 ng/mL and the upper bound was 6,000 ng/mL. Total accuracy ranged from 94.3–96.9%
528 for. Within-day coefficients of variation were below 5%, between-day coefficients of variation
529 were below 5%. Stability of 3TC in human plasma was also similar.

530

531 **Statistical analysis**

532 Baseline parameters were compared using Mann-Whitney tests for continuous variables and
533 Fisher's exact tests for categorical variables. Virological parameters were $\log_{10}$-transformed
534 before analysis. Longitudinal dynamics of the measured parameters was modelled using linear
535 mixed-effects analysis. This analysis was used both to compare the longitudinal changes from
536 baseline between the intensified and the control groups and to compare the changes from
537 baseline with zero in each of these groups separately (intercept-only analysis). As a sensitivity
538 analysis, we performed a comparison between models that do and do not include time as a
539 covariate. Including time in the models did not change the conclusions (Supplementary Tables
540 1 and 2). Paired Wilcoxon tests were used for within-group comparisons of parameters between
541 days 0 and 84. For these comparisons, pairs where both values were undetectable were
542 excluded from the analysis. Time-weighted changes from baseline were calculated by dividing
543 the areas under curve (computed using the trapezoid rule) by the time period of the study. Time-
544 weighted changes from baseline were not calculated if the baseline value and one or more of
545 the subsequent values were undetectable. Time-weighted changes from baseline and ratios of
546 the parameters between different study days were compared between the groups using Mann-
547 Whitney tests. Spearman tests were used to produce correlation matrices of the parameters at
548 baseline, as well as of time-weighted changes from baseline and of changes between day 0 and
549 day 84 of the measured parameters. Changes of the parameters from baseline, as well as US
550 RNA/total DNA ratios, were not calculated if both values in a pair were undetectable. Data

were analysed using Prism 10.2.0 (GraphPad Software) or IBM SPSS Statistics 28.0.1.0. All statistical tests were two-sided, and p values of <0.05 were considered statistically significant.

Acknowledgements

We are grateful to Marine Hubert and Raquel Mateus for technical assistance in PBMC isolation. We acknowledge the participation and commitment of the trial participants who made the study possible. C.F.L. is a FRIA grantee of the Belgian Fund for Scientific Research (Fonds de la Recherche Scientifique –FNRS) and is supported by the Fondation Léon Fredericq. This work was supported in part by grant R01-AI124965 (to C.V.F.) from the US National Institutes of Health. A.O.P. acknowledges grant support from amfAR, The Foundation for AIDS Research (grant no. 1110680–77-RPRL), and from Partnership NWO-Dutch AIDS Fonds 'HIV cure for everyone' (grant no. KICH2.V4P.AF23.001). G.D. is supported by the Belgian Fund for Scientific Research (Fonds de la Recherche Scientifique –FNRS).

References

1. Deeks SG, Lewin SR, Havlir DV. The end of AIDS: HIV infection as a chronic disease. Lancet. 2013;382(9903):1525-33.
2. Deeks SG, Overbaugh J, Phillips A, Buchbinder S. HIV infection. Nat Rev Dis Primers. 2015;1:15035.
3. Pasternak AO, Berkhout B. HIV persistence: silence or resistance? Curr Opin Virol. 2023;59:101301.
4. Darcis G, Berkhout B, Pasternak AO. The Quest for Cellular Markers of HIV Reservoirs: Any Color You Like. Front Immunol. 2019;10:2251.
5. De Scheerder MA, Vrancken B, Dellicour S, Schlub T, Lee E, Shao W, et al. HIV Rebound Is Predominantly Fueled by Genetically Identical Viral Expansions from Diverse Reservoirs. Cell Host Microbe. 2019;26(3):347-58.e7.
6. Siliciano JD, Kajdas J, Finzi D, Quinn TC, Chadwick K, Margolick JB, et al. Long-term follow-up studies confirm the stability of the latent reservoir for HIV-1 in resting CD4+ T cells. Nat Med. 2003;9(6):727-8.
7. Crooks AM, Bateson R, Cope AB, Dahl NP, Griggs MK, Kuruc JD, et al. Precise Quantitation of the Latent HIV-1 Reservoir: Implications for Eradication Strategies. J Infect Dis. 2015;212(9):1361-5.
8. Bachmann N, von Siebenthal C, Vongrad V, Turk T, Neumann K, Beerenwinkel N, et al. Determinants of HIV-1 reservoir size and long-term dynamics during suppressive ART. Nat Commun. 2019;10(1):3193.
9. Cohn LB, Chomont N, Deeks SG. The Biology of the HIV-1 Latent Reservoir and Implications for Cure Strategies. Cell Host Microbe. 2020;27(4):519-30.
10. Coffin JM, Hughes SH. Clonal Expansion of Infected CD4+ T Cells in People Living with HIV. Viruses. 2021;13(10).

591 11. Chun TW, Nickle DC, Justement JS, Large D, Semerjian A, Curlin ME, et al. HIV-infected
592 individuals receiving effective antiviral therapy for extended periods of time continually replenish their
593 viral reservoir. J Clin Invest. 2005;115(11):3250-5.
594 12. Martinez-Picado J, Deeks SG. Persistent HIV-1 replication during antiretroviral therapy. Curr
595 Opin HIV AIDS. 2016;11(4):417-23.
596 13. Sigal A, Kim JT, Balazs AB, Dekel E, Mayo A, Milo R, et al. Cell-to-cell spread of HIV permits
597 ongoing replication despite antiretroviral therapy. Nature. 2011;477(7362):95-8.
598 14. Lorenzo-Redondo R, Fryer HR, Bedford T, Kim EY, Archer J, Pond SLK, et al. Persistent HIV-
599 1 replication maintains the tissue reservoir during therapy. Nature. 2016;530(7588):51-6.
600 15. Pasternak AO, de Bruin M, Jurriaans S, Bakker M, Berkhout B, Prins JM, et al. Modest
601 nonadherence to antiretroviral therapy promotes residual HIV-1 replication in the absence of virological
602 rebound in plasma. J Infect Dis. 2012;206(9):1443-52.
603 16. Pasternak AO, Vroom J, Kootstra NA, Wit FW, de Bruin M, De Francesco D, et al. Non-
604 nucleoside reverse transcriptase inhibitor-based combination antiretroviral therapy is associated with
605 lower cell-associated HIV RNA and DNA levels as compared with therapy based on protease inhibitors.
606 Elife. 2021;10:e68174.
607 17. Bozzi G, Simonetti FR, Watters SA, Anderson EM, Gouzoulis M, Kearney MF, et al. No
608 evidence of ongoing HIV replication or compartmentalization in tissues during combination
609 antiretroviral therapy: Implications for HIV eradication. Sci Adv. 2019;5(9):eaav2045.
610 18. Kearney MF, Wiegand A, Shao W, McManus WR, Bale MJ, Luke B, et al. Ongoing HIV
611 Replication During ART Reconsidered. Open Forum Infectious Diseases. 2017;4(3):ofx173.
612 19. Van Zyl GU, Katusiime MG, Wiegand A, McManus WR, Bale MJ, Halvas EK, et al. No
613 evidence of HIV replication in children on antiretroviral therapy. J Clin Invest. 2017;127(10):3827-34.
614 20. Kearney MF, Spindler J, Shao W, Yu S, Anderson EM, O'Shea A, et al. Lack of detectable HIV-
615 1 molecular evolution during suppressive antiretroviral therapy. PLoS Pathog. 2014;10(3):e1004010.
616 21. Conway JM, Perelson AS. Residual Viremia in Treated HIV+ Individuals. PLoS Comput Biol.
617 2016;12(1):e1004677.
618 22. Paryad-Zanjani S, Jagarapu A, Piovoso MJ, Zurakowski R. Ongoing HIV replication in lymph
619 node sanctuary sites in treated individuals contributes to the total latent HIV at a very slow rate. J Theor
620 Biol. 2023;575:111651.
621 23. Zicari S, Sessa L, Cotugno N, Ruggiero A, Morrocchi E, Concato C, et al. Immune Activation,
622 Inflammation, and Non-AIDS Co-Morbidities in HIV-Infected Patients under Long-Term ART. Viruses.
623 2019;11(3).
624 24. Mazzuti L, Turriziani O, Mezzaroma I. The Many Faces of Immune Activation in HIV-1
625 Infection: A Multifactorial Interconnection. Biomedicines. 2023;11(1).
626 25. Chun TW, Nickle DC, Justement JS, Meyers JH, Roby G, Hallahan CW, et al. Persistence of
627 HIV in gut-associated lymphoid tissue despite long-term antiretroviral therapy. J Infect Dis.
628 2008;197(5):714-20.
629 26. Fletcher CV, Staskus K, Wietgrefe SW, Rothenberger M, Reilly C, Chipman JG, et al. Persistent
630 HIV-1 replication is associated with lower antiretroviral drug concentrations in lymphatic tissues. Proc
631 Natl Acad Sci U S A. 2014;111(6):2307-12.
632 27. Fletcher CV, Kroon E, Schacker T, Pinyakorn S, Chomont N, Chottanapund S, et al. Persistent
633 HIV transcription and variable antiretroviral drug penetration in lymph nodes during plasma viral
634 suppression. AIDS. 2022;36(7):985-90.
635 28. Estes JD, Kityo C, Ssali F, Swainson L, Makamdop KN, Del Prete GQ, et al. Defining total-
636 body AIDS-virus burden with implications for curative strategies. Nat Med. 2017;23(11):1271-1276.
637 29. Havlir DV, Strain MC, Clerici M, Ignacio C, Trabattoni D, Ferrante P, et al. Productive infection
638 maintains a dynamic steady state of residual viremia in human immunodeficiency virus type 1-infected
639 persons treated with suppressive antiretroviral therapy for five years. J Virol. 2003;77(20):11212-9.
640 30. Ramratnam B, Ribeiro R, He T, Chung C, Simon V, Vanderhoeven J, et al. Intensification of
641 antiretroviral therapy accelerates the decay of the HIV-1 latent reservoir and decreases, but does not
642 eliminate, ongoing virus replication. J Acquir Immune Defic Syndr. 2004;35(1):33-7.
643 31. Buzon MJ, Massanella M, Llibre JM, Esteve A, Dahl V, Puertas MC, et al. HIV-1 replication
644 and immune dynamics are affected by raltegravir intensification of HAART-suppressed subjects. Nat
645 Med. 2010;16(4):460-5.

646 32. Yukl SA, Shergill AK, McQuaid K, Gianella S, Lampiris H, Hare CB, et al. Effect of raltegravir-
647 containing intensification on HIV burden and T-cell activation in multiple gut sites of HIV-positive
648 adults on suppressive antiretroviral therapy. AIDS. 2010;24(16):2451-60.
649 33. Llibre JM, Buzon MJ, Massanella M, Esteve A, Dahl V, Puertas MC, et al. Treatment
650 intensification with raltegravir in subjects with sustained HIV-1 viraemia suppression: a randomized
651 48-week study. Antivir Ther. 2012;17(2):355-64.
652 34. Vallejo A, Gutierrez C, Hernandez-Novoa B, Diaz L, Madrid N, Abad-Fernandez M, et al. The
653 effect of intensification with raltegravir on the HIV-1 reservoir of latently infected memory CD4 T cells
654 in suppressed patients. AIDS. 2012;26(15):1885-94.
655 35. Gutierrez C, Diaz L, Vallejo A, Hernandez-Novoa B, Abad M, Madrid N, et al. Intensification
656 of antiretroviral therapy with a CCR5 antagonist in patients with chronic HIV-1 infection: effect on T
657 cells latently infected. PLoS One. 2011;6(12):e27864.
658 36. Hatano H, Strain MC, Scherzer R, Bacchetti P, Wentworth D, Hoh R, et al. Increase in 2-long
659 terminal repeat circles and decrease in D-dimer after raltegravir intensification in patients with treated
660 HIV infection: a randomized, placebo-controlled trial. J Infect Dis. 2013;208(9):1436-42.
661 37. Puertas MC, Gómez-Mora E, Santos JR, Moltó J, Urrea V, Morón-López S, et al. Impact of
662 intensification with raltegravir on HIV-1-infected individuals receiving monotherapy with boosted PIs.
663 J Antimicrob Chemother. 2018;73(7):1940-8.
664 38. Puertas MC, Massanella M, Llibre JM, Ballestero M, Buzon MJ, Ouchi D, et al. Intensification
665 of a raltegravir-based regimen with maraviroc in early HIV-1 infection. AIDS. 2014;28(3):325-34.
666 39. Dinoso JB, Kim SY, Wiegand AM, Palmer SE, Gange SJ, Cranmer L, et al. Treatment
667 intensification does not reduce residual HIV-1 viremia in patients on highly active antiretroviral therapy.
668 Proc Natl Acad Sci U S A. 2009;106(23):9403-8.
669 40. McMahon D, Jones J, Wiegand A, Gange SJ, Kearney M, Palmer S, et al. Short-course
670 raltegravir intensification does not reduce persistent low-level viremia in patients with HIV-1
671 suppression during receipt of combination antiretroviral therapy. Clin Infect Dis. 2010;50(6):912-9.
672 41. Gandhi RT, Coombs RW, Chan ES, Bosch RJ, Zheng L, Margolis DM, et al. No effect of
673 raltegravir intensification on viral replication markers in the blood of HIV-1-infected patients receiving
674 antiretroviral therapy. J Acquir Immune Defic Syndr. 2012;59(3):229-35.
675 42. Gandhi RT, Zheng L, Bosch RJ, Chan ES, Margolis DM, Read S, et al. The effect of raltegravir
676 intensification on low-level residual viremia in HIV-infected patients on antiretroviral therapy: a
677 randomized controlled trial. PLoS Med. 2010;7(8).
678 43. Cillo AR, Hilldorfer BB, Lalama CM, McKinnon JE, Coombs RW, Tenorio AR, et al. Virologic
679 and immunologic effects of adding maraviroc to suppressive antiretroviral therapy in individuals with
680 suboptimal CD4+ T-cell recovery. AIDS. 2015;29(16):2121-9.
681 44. Chaillon A, Gianella S, Lada SM, Perez-Santiago J, Jordan P, Ignacio C, et al. Size,
682 Composition, and Evolution of HIV DNA Populations during Early Antiretroviral Therapy and
683 Intensification with Maraviroc. J Virol. 2018;92(3).
684 45. Rasmussen TA, McMahon JH, Chang JJ, Audsley J, Rhodes A, Tennakoon S, et al. The effect
685 of antiretroviral intensification with dolutegravir on residual virus replication in HIV-infected
686 individuals: a randomised, placebo-controlled, double-blind trial. Lancet HIV. 2018;5(5):e221-e30.
687 46. Deeks SG. HIV: Shock and kill. Nature. 2012;487(7408):439-40.
688 47. Greener BN, Patterson KB, Prince HM, Sykes CS, Adams JL, Dumond JB, et al. Dolutegravir
689 pharmacokinetics in the genital tract and colorectum of HIV-negative men after single and multiple
690 dosing. J Acquir Immune Defic Syndr. 2013;64(1):39-44.
691 48. Podsadecki TJ, Vrijens BC, Tousset EP, Rode RA, Hanna GJ. "White coat compliance" limits
692 the reliability of therapeutic drug monitoring in HIV-1-infected patients. HIV Clin Trials.
693 2008;9(4):238-46.
694 49. Bruner KM, Wang Z, Simonetti FR, Bender AM, Kwon KJ, Sengupta S, et al. A quantitative
695 approach for measuring the reservoir of latent HIV-1 proviruses. Nature. 2019;566(7742):120-5.
696 50. Scherpenisse M, Kootstra NA, Bakker M, Berkhout B, Pasternak AO. Cell-Associated HIV-1
697 Unspliced-to-Multiply-Spliced RNA Ratio at 12 Weeks of ART Predicts Immune Reconstitution on
698 Therapy. mBio. 2021;12(2).

699 51. Peluso MJ, Bacchetti P, Ritter KD, Beg S, Lai J, Martin JN, et al. Differential decay of intact
700 and defective proviral DNA in HIV-1-infected individuals on suppressive antiretroviral therapy. JCI
701 Insight. 2020;5(4).
702 52. Gandhi RT, Cyktor JC, Bosch RJ, Mar H, Laird GM, Martin A, et al. Selective Decay of Intact
703 HIV-1 Proviral DNA on Antiretroviral Therapy. J Infect Dis. 2021;223(2):225-33.
704 53. Chew GM, Fujita T, Webb GM, Burwitz BJ, Wu HL, Reed JS, et al. TIGIT Marks Exhausted T
705 Cells, Correlates with Disease Progression, and Serves as a Target for Immune Restoration in HIV and
706 SIV Infection. PLoS Pathog. 2016;12(1):e1005349.
707 54. Fromentin R, Bakeman W, Lawani MB, Khoury G, Hartogensis W, DaFonseca S, et al. CD4+
708 T Cells Expressing PD-1, TIGIT and LAG-3 Contribute to HIV Persistence during ART. PLoS Pathog.
709 2016;12(7):e1005761.
710 55. Darcis G, Maes N, Pasternak AO, Sauvage AS, Frippiat F, Meuris C, et al. Detectability of HIV
711 Residual Viremia despite Therapy Is Highly Associated with Treatment with a Protease Inhibitor-Based
712 Combination Antiretroviral Therapy. Antimicrob Agents Chemother. 2020;64(3).
713 56. Darcis G, Berkhout B, Pasternak AO. Differences in HIV Markers between Infected Individuals
714 Treated with Different ART Regimens: Implications for the Persistence of Viral Reservoirs. Viruses.
715 2020;12(5).
716 57. Hatano H, Hayes TL, Dahl V, Sinclair E, Lee TH, Hoh R, et al. A randomized, controlled trial
717 of raltegravir intensification in antiretroviral-treated, HIV-infected patients with a suboptimal CD4+ T
718 cell response. J Infect Dis. 2011;203(7):960-8.
719 58. Butler SL, Hansen MS, Bushman FD. A quantitative assay for HIV DNA integration in vivo.
720 Nat Med. 2001;7(5):631-4.
721 59. Hockett RD, Kilby JM, Derdeyn CA, Saag MS, Sillers M, Squires K, et al. Constant mean viral
722 copy number per infected cell in tissues regardless of high, low, or undetectable plasma HIV RNA. J
723 Exp Med. 1999;189(10):1545-54.
724 60. Rothenberger M, Nganou-Makamdop K, Kityo C, Ssali F, Chipman JG, Beilman GJ, et al.
725 Impact of Integrase Inhibition compared to non-nucleoside inhibition on HIV reservoirs in Lymphoid
726 Tissues. J Acquir Immune Defic Syndr. 2019.
727 61. Lee SA, Telwatte S, Hatano H, Kashuba ADM, Cottrell ML, Hoh R, et al. Antiretroviral
728 Therapy Concentrations Differ in Gut vs. Lymph Node Tissues and Are Associated With HIV Viral
729 Transcription by a Novel RT-ddPCR Assay. J Acquir Immune Defic Syndr. 2020;83(5):530-7.
730 62. Galloway NL, Doitsh G, Monroe KM, Yang Z, Muñoz-Arias I, Levy DN, et al. Cell-to-Cell
731 Transmission of HIV-1 Is Required to Trigger Pyroptotic Death of Lymphoid-Tissue-Derived CD4 T
732 Cells. Cell Rep. 2015;12(10):1555-63.
733 63. Doitsh G, Cavrois M, Lassen KG, Zepeda O, Yang Z, Santiago ML, et al. Abortive HIV
734 infection mediates CD4 T cell depletion and inflammation in human lymphoid tissue. Cell.
735 2010;143(5):789-801.
736 64. Boom R, Sol CJ, Salimans MM, Jansen CL, Wertheim-van Dillen PM, van der Noordaa J.
737 Rapid and simple method for purification of nucleic acids. J Clin Microbiol. 1990;28(3):495-503.
738 65. Malnati MS, Scarlatti G, Gatto F, Salvatori F, Cassina G, Rutigliano T, et al. A universal real-
739 time PCR assay for the quantification of group-M HIV-1 proviral load. Nat Protoc. 2008;3(7):1240-8.
740 66. Pasternak AO, Jurriaans S, Bakker M, Prins JM, Berkhout B, Lukashov VV. Cellular levels of
741 HIV unspliced RNA from patients on combination antiretroviral therapy with undetectable plasma
742 viremia predict the therapy outcome. PLoS One. 2009;4(12):e8490.
743 67. Fischer M, Huber W, Kallivroussis A, Ott P, Opravil M, Luthy R, et al. Highly sensitive methods
744 for quantitation of human immunodeficiency virus type 1 RNA from plasma, cells, and tissues. J Clin
745 Microbiol. 1999;37(5):1260-4.
746 68. Levy CN, Hughes SM, Roychoudhury P, Reeves DB, Amstuz C, Zhu H, et al. A highly
747 multiplexed droplet digital PCR assay to measure the intact HIV-1 proviral reservoir. Cell Rep Med.
748 2021;2(4):100243.
749 69. Luo W, Yang H, Rathbun K, Pau CP, Ou CY. Detection of human immunodeficiency virus type
750 1 DNA in dried blood spots by a duplex real-time PCR assay. J Clin Microbiol. 2005;43(4):1851-7.
751 70. Fletcher CV, Podany AT, Thorkelson A, Winchester LC, Mykris T, Anderson J, et al. The
752 Lymphoid Tissue Pharmacokinetics of Tenofovir Disoproxil Fumarate and Tenofovir Alafenamide in
753 HIV-Infected Persons. Clin Pharmacol Ther. 2020;108(5):971-5.

754 71. Dyavar SR, Kumar S, Gautam N, Podany AT, Winchester LC, Weinhold JA, et al. Intramuscular
755 and subcutaneous administration of antiretroviral drugs, compared with oral, enhances delivery to
756 lymphoid tissues in BALB/c mice. J Antimicrob Chemother. 2021;76(10):2651-8.
757 72. Delahunty T, Bushman L, Fletcher CV. Sensitive assay for determining plasma tenofovir
758 concentrations by LC/MS/MS. J Chromatogr B Analyt Technol Biomed Life Sci. 2006;830(1):6-12.

759

760

761 **Figure legends**

762 **Figure 1**. Antiretroviral drug concentrations in plasma and rectal tissue. Plasma (A) and tissue
763 (B) concentrations of DTG, as well as plasma (C) and tissue (D) concentrations of 3TC, were
764 compared between days 0 (D0) and 84 (D84) in intensified and control groups. Wilcoxon tests
765 were used to calculate statistical significance.

766 **Figure 2**. Longitudinal dynamics of HIV reservoir markers. (A-C) Fold change of total HIV
767 DNA in PBMCs (A), US HIV RNA in PBMCs (B), and US RNA/total DNA ratios (C) from
768 baseline on days 1, 28, 56, and 84 of the study in the intensified (blue) and control (red) groups.
769 Median values and IQRs are shown. Linear mixed-effects modelling on log_{10}-transformed
770 values was used to calculate statistical significance. P values at the bottom of the graphs show
771 the significance of between-group comparisons and those on top of the graphs show the
772 significance of comparisons of the changes from baseline with zero in each group separately
773 (intercept-only analysis). An upward or downward facing arrow next to a p value indicates a
774 statistically significant increase or decrease from baseline, respectively. Participant numbers in
775 both groups per time point are indicated below the graphs. (D, E) Comparisons of intact HIV
776 DNA in PBMCs (D) and of total HIV DNA in rectal tissue (E) between days 0 (D0) and 84
777 (D84) in the intensified and control groups. Open circles depict undetectable values, assigned
778 the values corresponding to 50% of the assay detection limits. Wilcoxon tests were used to
779 calculate statistical significance. All p values are marked red if significant (<0.05).

780 **Figure 3**. Longitudinal dynamics of cellular markers of immune activation and exhaustion.
781 Graphs show changes of (A) CD4+ cell markers and (B) CD8+ cell markers from baseline on
782 days 1, 28, 56, and 84 of the study in the intensified (blue) and control (red) groups. Median
783 values and IQRs are shown. Linear mixed-effects modelling was used to calculate statistical
784 significance. P values at the bottom of the graphs show the significance of between-group
785 comparisons and those on top of the graphs show the significance of comparisons of the
786 changes from baseline with zero in each group separately (intercept-only analysis). An upward
787 or downward facing arrow next to a p value indicates a statistically significant increase or
788 decrease from baseline, respectively. P values are marked red if significant (<0.05).

789 **Figure 4**. Longitudinal dynamics of inflammation markers in plasma and tissue. (A) Plasma
790 inflammation markers. Graphs show changes of markers from baseline on days 1, 28, 56, and
791 84 of the study in the intensified (blue) and control (red) groups. Median values and IQRs are
792 shown. Linear mixed-effects modelling was used to calculate statistical significance. P values

793 at the bottom of the graphs show the significance of between-group comparisons and those on
794 top of the graphs show the significance of comparisons of the changes from baseline with zero
795 in each group separately (intercept-only analysis). An upward or downward facing arrow next
796 to a p value indicates a statistically significant increase or decrease from baseline, respectively.
797 P values are marked red if significant (<0.05). (B) Tissue inflammation markers. Markers were
798 compared between days 0 (D0) and 84 (D84) in the intensified and control groups. Open circles
799 depict undetectable values, assigned the values corresponding to 50% of the assay detection
800 limits. Wilcoxon tests were used to calculate statistical significance.

801 **Figure 5**. Longitudinal dynamics of clinical markers. Graphs show changes of markers from
802 baseline on days 1, 28, 56, and 84 of the study in the intensified (blue) and control (red) groups.
803 Median values and IQRs are shown. Linear mixed-effects modelling was used to calculate
804 statistical significance. P values at the bottom of the graphs show the significance of between-
805 group comparisons and those on top of the graphs show the significance of comparisons of the
806 changes from baseline with zero in each group separately (intercept-only analysis). An upward
807 or downward facing arrow next to a p value indicates a statistically significant increase or
808 decrease from baseline, respectively. P values are marked red if significant (<0.05).

809

Table 1. Clinical characteristics of participants at baseline.

	All (n=20)	Control group (n=10)	DTG group (n=10)	p[a]
Sex, male	19 (95.0)[b]	9 (90.0)	10 (100.0)	1.00
Age, years	52 (43-60; 25-73)	52 (40-62; 25-73)	51 (46-59; 36-66)	0.94
BMI, kg/m²	24 (22-26; 18-36)	25 (22-27; 19-30)	23 (22-26; 18-36)	0.62
Ethnicity				
Caucasian	17 (85.0)	9 (90.0)	8 (80.0)	1.00
African	2 (10.0)	1 (10.0)	1 (10.0)	
Maghrebi	1 (5.0)	0 (0.0)	1 (10.0)	
HLA typing B57/01, negative (n=19)	19 (100.0)	9 (100.0)	10 (100.0)	-
Smoking, smoker or ex-smoker	10 (50.0)	4 (40.0)	6 (60.0)	0.66
Time since first positive HIV serology, years	12.6 (6.8-18.2; 3.5-25.4)	9.8 (7.3-13.3; 3.5-25.4)	15.6 (7.6-18.5; 3.5-21.5)	0.58
Cumulative time of untreated HIV infection, years	0.9 (0.1-3.5; 0.0-17.2)	1.8 (0.1-5.0; 0.0-17.2)	0.6 (0.1-2.1; 0.0-6.1)	0.47
Cumulative time of viral suppression, years	7.4 (4.8-9.2; 2.9-16.5)	5.6 (4.7-7.7; 3.3-16.2)	7.9 (5.8-12.4; 2.9-16.5)	0.32
Continuous time of viral suppression before study, years	3.9 (3.3-5.8; 0.4-10.2)	4.4 (3.7-6.9; 3.3-10.2)	3.4 (3.2-4.9; 0.4-7.9)	0.12
Time on DTG-containing ART regimen before study, years	3.5 (3.4-3.7; 2.2-3.9)	3.5 (3.4-3.8; 2.2-3.9)	3.5 (3.3-3.5; 2.7-3.8)	0.41
Nadir CD4+ count, cells/mm³	277 (147-410; 24-747)	277 (205-340; 24-521)	292 (136-508; 30-747)	0.65
First measured plasma viral load, log_{10} HIV RNA copies/mL	4.52 (3.91-5.35; 2.48-6.60)	4.52 (4.36-4.96; 3.00-6.60)	4.55 (3.69-5.38; 2.48-5.70)	0.85
CD4+ count, cells/mm³	775 (659-1144; 225-1383)	732 (672-970; 225-1267)	886 (668-1217; 492-1383)	0.39
CD8+ count, cells/mm³	745 (637-1288; 377-2017)	723 (535-931; 377-2017)	939 (690-1310; 501-1853)	0.39
CD4/CD8 ratio	0.94 (0.66-1.47; 0.32-2.24)	1.00 (0.64-1.36; 0.32-1.82)	0.93 (0.69-1.56; 0.35-2.24)	0.82
Total HIV DNA in PBMCs, copies/10^6 cells	175.5 (70.0-467.3; 15.1-1090)	99.4 (37.4-231.5; 15.1-333.0)	421.0 (139.5-764.3; 61.8-1090)	0.015
Intact HIV DNA in PBMCs, copies/10^6 cells	55.2 (19.2-87.0; 5.17-624.2)	29.5 (16.2-97.1; 10.3-624.2)	58.6 (44.7-144.7; 5.17-292.6)	0.36
US HIV RNA in PBMCs, copies/µg total RNA	92.1 (13.3-290.3; 2.53-1580)	72.2 (12.2-253.8; 6.18-486)	124.6 (17.0-591.0; 2.53-1580)	0.58
US RNA/total DNA ratio in PBMCs	0.40 (0.07-1.47; 0.03-3.96)	1.21 (0.11-2.81; 0.04-3.96)	0.33 (0.06-0.70; 0.03-2.73)	0.21
Total HIV DNA in rectal tissue, copies/10^6 cells	477.0 (271.3-971.5; 7.27-1720)	547.0 (291.0-1215; 53.4-1720)	403.0 (194.6-952.5; 7.27-1510)	0.44
Plasma DTG concentration, ng/mL	3287 (2602-5087; 237-6593)	3560 (2953-4455; 1969-5536)	3266 (2245-5983; 237-6593)	0.82
Tissue DTG concentration, ng/g	634 (533-830; 303-1810)	737 (534-852; 482-1810)	581 (535-714; 303-1037)	0.44
Plasma 3TC concentration, ng/mL	316 (148-731; 50-1616)	431 (214-941; 102-1616)	246 (117-439; 50-1156)	0.26
Tissue 3TC concentration, ng/g	2114 (1417-2345; 90-4495)	2193 (1590-2784; 1215-4495)	2114 (1233-2317; 900-3187)	0.50
CDC classification				-
A1	4 (20.0)	1 (10.0)	3 (30.0)	
A2	9 (45.0)	6 (60.0)	3 (30.0)	
A3	3 (15.0)	1 (10.0)	2 (30.0)	
B3	1 (5.0)	0 (0.0)	1 (10.0)	
C3	3 (15.0)	2 (20.0)	1 (10.0)	
HBV status				-
Immune	12 (60.0)	8 (80.0)	4 (40.0)	
Non-immune, not infected	5 (25.0)	2 (20.0)	3 (30.0)	
Isolated HBc Ab	2 (10.0)	0 (0.0)	2 (20.0)	

Cured Hepatitis B	1 (5.0)	0 (0.0)	1 (10.0)	
HCV status				1.00
Not Infected	19 (95.0)	10 (10.0)	9 (90.0)	
Recovered	1 (5.0)	0 (0.0)	1 (10.0)	

811

812

813

[a] Mann-Whitney tests were used for continuous variables and Fisher's exact tests were used for categorical variables.
[b] Data are medians (interquartile ranges, followed by ranges) for continuous variables and numbers (percentages) for discrete variables.

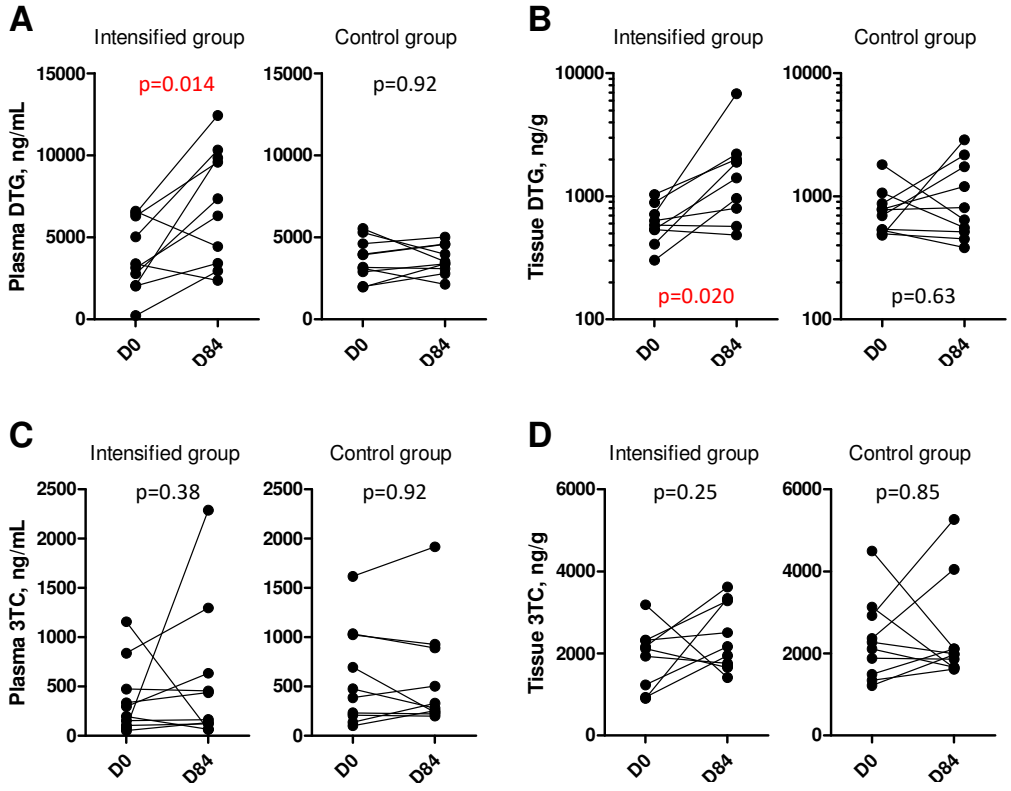

Figure 1. Antiretroviral drug concentrations in plasma and rectal tissue. Plasma (A) and tissue (B) concentrations of DTG, as well as plasma (C) and tissue (D) concentrations of 3TC, were compared between days 0 (D0) and 84 (D84) in intensified and control groups. Wilcoxon tests were used to calculate statistical significance.

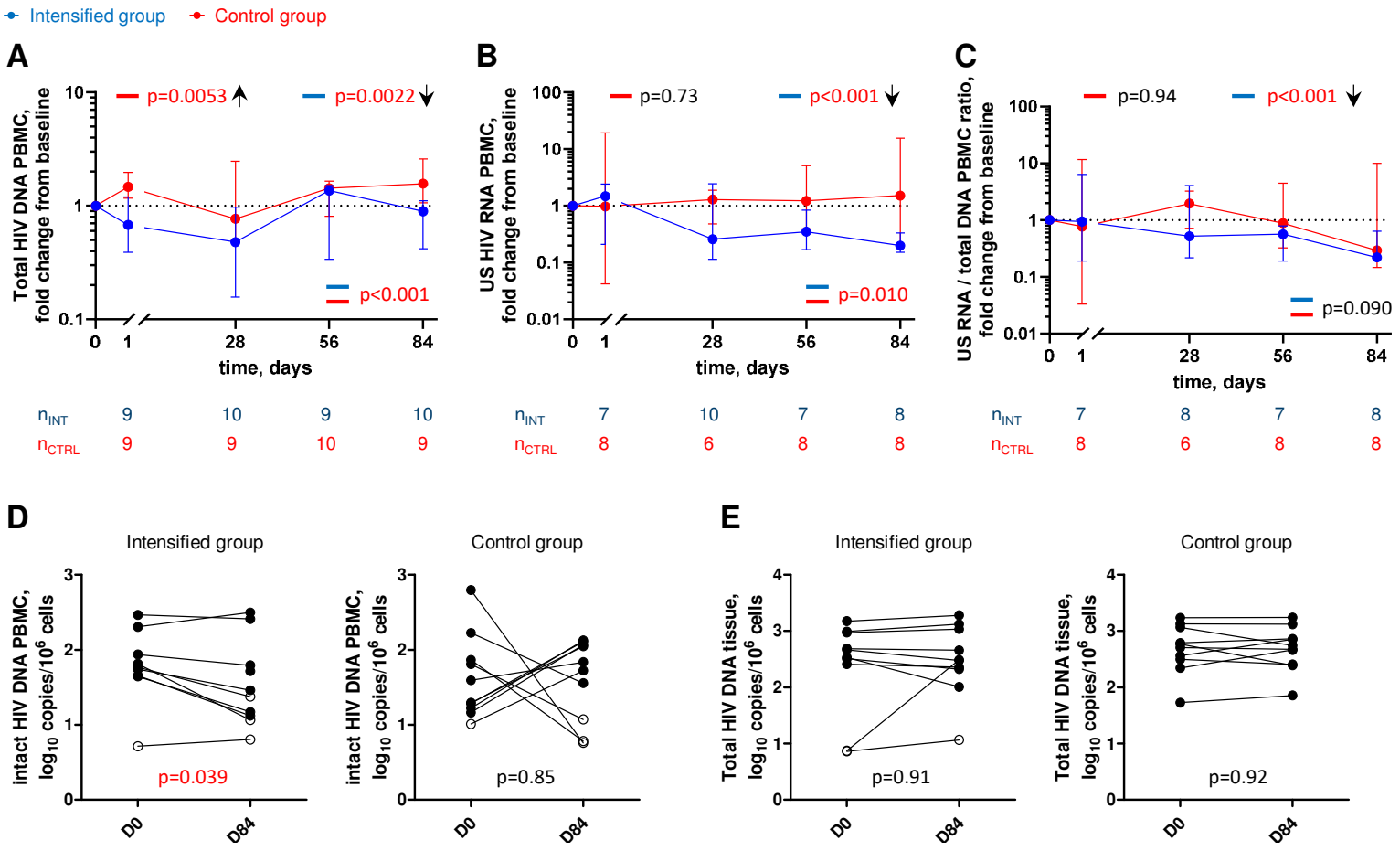

Figure 2. Longitudinal dynamics of HIV reservoir markers. (A-C) Fold change of total HIV DNA in PBMCs (A), US HIV RNA in PBMCs (B), and US RNA/total DNA ratios (C) from baseline on days 1, 28, 56, and 84 of the study in the intensified (blue) and control (red) groups. Median values and IQRs are shown. Linear mixed-effects modelling on log10-transformed values was used to calculate statistical significance. P values at the bottom of the graphs show the significance of between-group comparisons and those on top of the graphs show the significance of comparisons of the changes from baseline with zero in each group separately (intercept-only analysis). An upward or downward facing arrow next to a p value indicates a statistically significant increase or decrease from baseline, respectively. Participant numbers in both groups per time point are indicated below the graphs. (D, E) Comparisons of intact HIV DNA in PBMCs (D) and of total HIV DNA in rectal tissue (E) between days 0 (D0) and 84 (D84) in the intensified and control groups. Open circles depict undetectable values, assigned the values corresponding to 50% of the assay detection limits. Wilcoxon tests were used to calculate statistical significance. All p values are marked red if significant (<0.05).

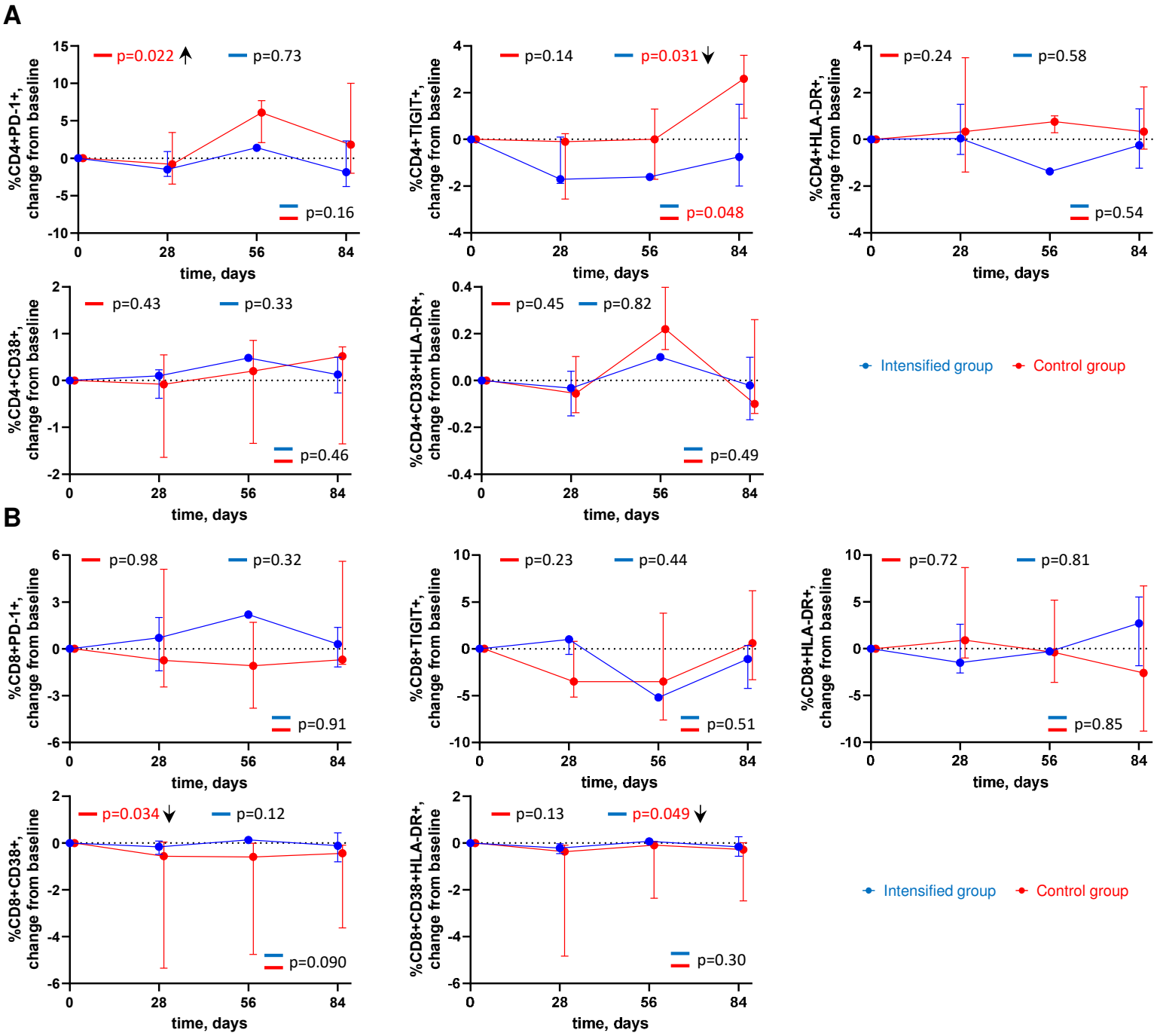

Figure 3. Longitudinal dynamics of cellular markers of immune activation and exhaustion. Graphs show changes of (A) CD4+ cell markers and (B) CD8+ cell markers from baseline on days 1, 28, 56, and 84 of the study in the intensified (blue) and control (red) groups. Median values and IQRs are shown. Linear mixed-effects modelling was used to calculate statistical significance. P values at the bottom of the graphs show the significance of between-group comparisons and those on top of the graphs show the significance of comparisons of the changes from baseline with zero in each group separately (intercept-only analysis). An upward or downward facing arrow next to a p value indicates a statistically significant increase or decrease from baseline, respectively. P values are marked red if significant (<0.05).

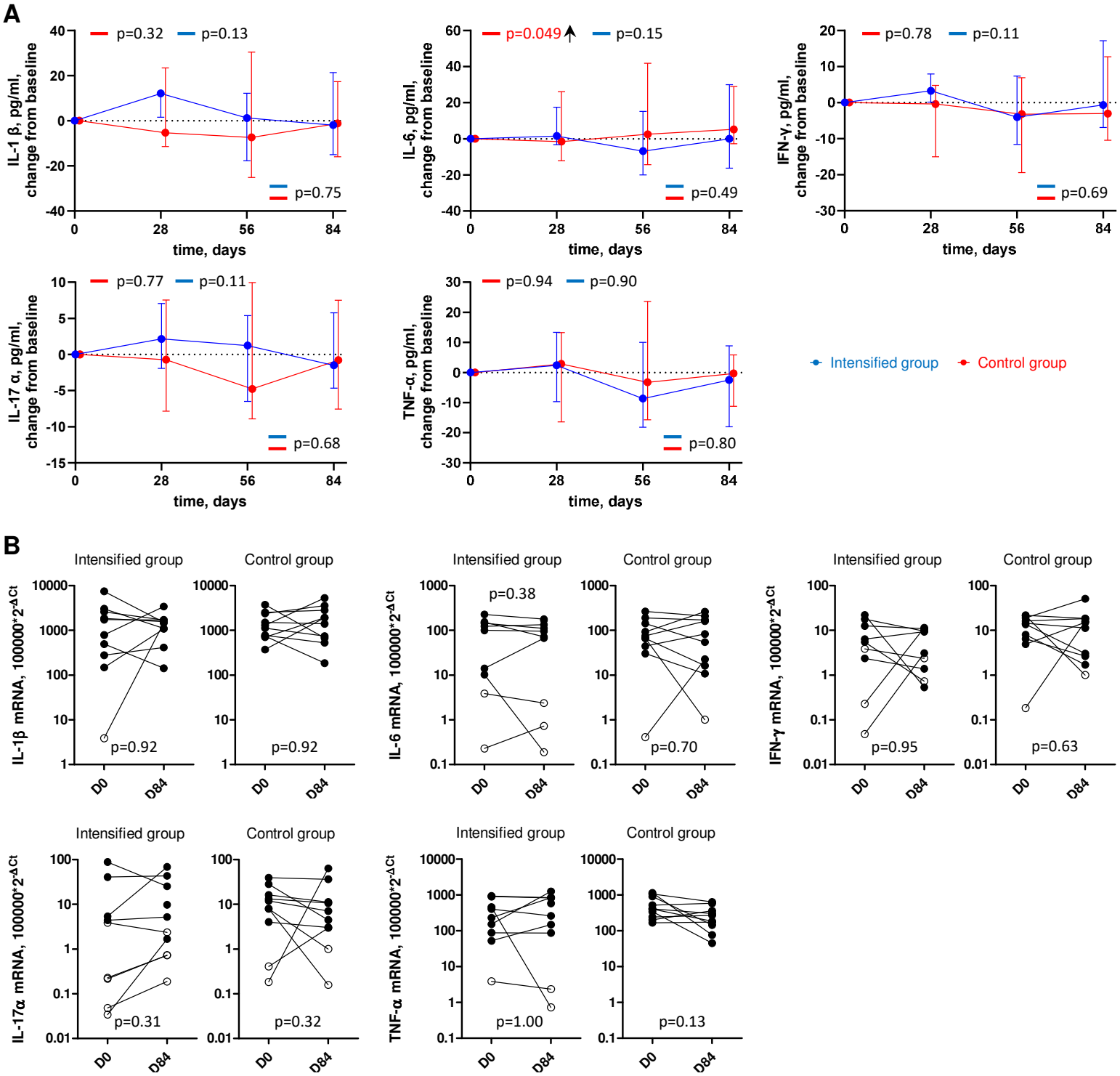

Figure 4. Longitudinal dynamics of inflammation markers in plasma and tissue. (A) Plasma inflammation markers. Graphs show changes of markers from baseline on days 1, 28, 56, and 84 of the study in the intensified (blue) and control (red) groups. Median values and IQRs are shown. Linear mixed-effects modelling was used to calculate statistical significance. P values at the bottom of the graphs show the significance of between-group comparisons and those on top of the graphs show the significance of comparisons of the changes from baseline with zero in each group separately (intercept-only analysis). An upward or downward facing arrow next to a p value indicates a statistically significant increase or decrease from baseline, respectively. P values are marked red if significant (<0.05). (B) Tissue inflammation markers. Markers were compared between days 0 (D0) and 84 (D84) in the intensified and control groups. Open circles depict undetectable values, assigned the values corresponding to 50% of the assay detection limits. Wilcoxon tests were used to calculate statistical significance.

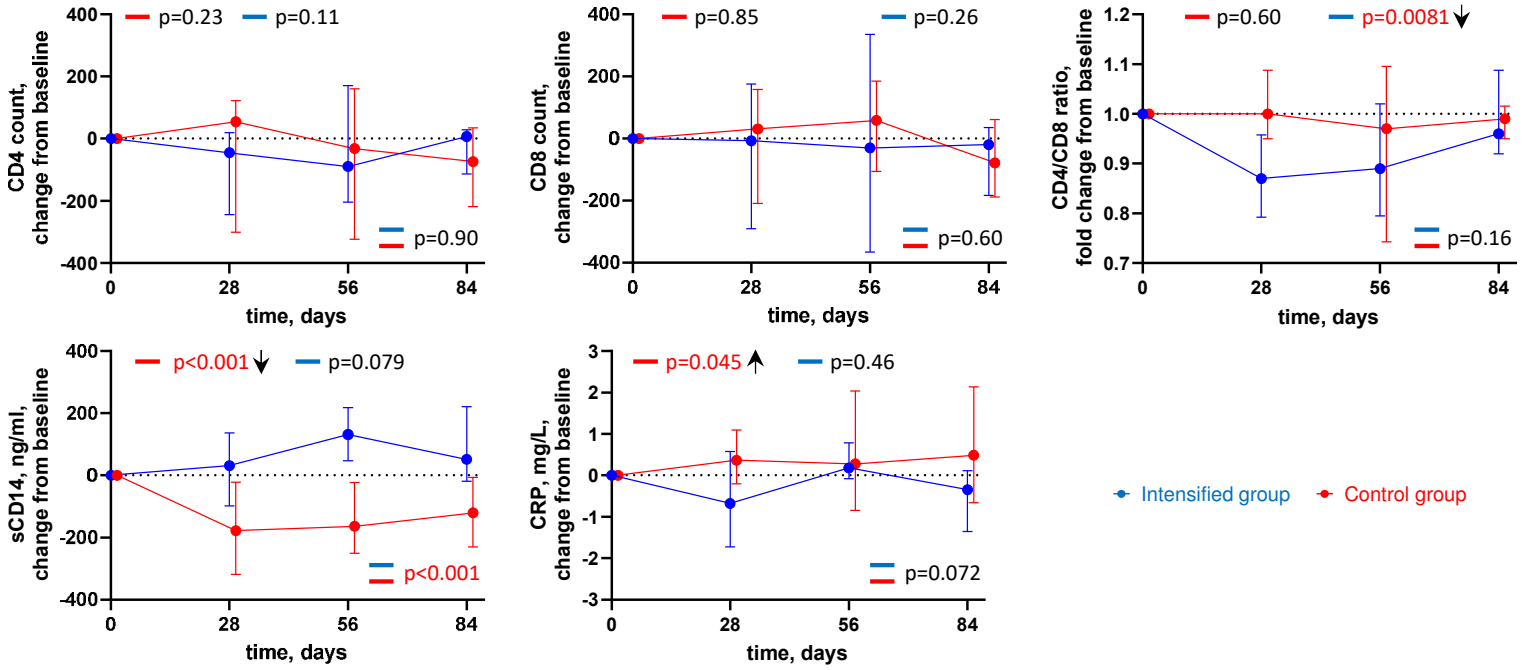

Figure 5. Longitudinal dynamics of clinical markers. Graphs show changes of markers from baseline on days 1, 28, 56, and 84 of the study in the intensified (blue) and control (red) groups. Median values and IQRs are shown. Linear mixed-effects modelling was used to calculate statistical significance. P values at the bottom of the graphs show the significance of between-group comparisons and those on top of the graphs show the significance of comparisons of the changes from baseline with zero in each group separately (intercept-only analysis). An upward or downward facing arrow next to a p value indicates a statistically significant increase or decrease from baseline, respectively. P values are marked red if significant (<0.05).